



Identification of Egyptian Mangrove Species Based on DNA Barcoding

Eglal M. Said ^{a*} and M. I. Bahnasy ^b

^a Breeding Research Department of Fruit Trees, Ornamental and Woody Plants, Horticulture Research Institute, ARC, Giza, Egypt.

^b Forestry and Timber Trees Department, Horticulture Research Institute, ARC, Giza, Egypt.

Authors' contributions

This work was carried out in collaboration between both authors. Both authors read and approved the final manuscript.

Article Information

DOI: 10.9734/AJAHR/2023/v10i4254

Open Peer Review History:

This journal follows the Advanced Open Peer Review policy. Identity of the Reviewers, Editor(s) and additional Reviewers, peer review comments, different versions of the manuscript, comments of the editors, etc are available here: <https://www.sdiarticle5.com/review-history/100871>

Original Research Article

Received: 01/04/2023

Accepted: 03/06/2023

Published: 17/06/2023

ABSTRACT

Aims: Mangroves are woody trees or shrubs that grow in the intertidal zone and are distributed along tropical and subtropical coasts. These plants are resilient to various environmental challenges; they are also one of the most efficient terrestrial and coastal ecosystem for carbon fixation and storage. In recent years, mangrove reforestation has attracted much attention as a strategy to reduce the effects of climate change. In Egypt, there are two types of mangroves, *Rhizophora mucronata* and *Avicennia marina*, between 30°N and 30°S of the equator. Mangrove management presents a difficult task, particularly when it comes to managing molecular mangroves for long-term sustainability. With the impact of human activity on mangrove ecosystems increasing each year, molecular research on mangrove correlates remains to be conducted. For this reason, using DNA barcoding technology to quickly identify species, mangrove ecosystems may be protected.

Methodology: In this work, the two Egyptian mangrove species were assessed through morphological, cytological, and molecular approaches. Two universal DNA barcodes, *rbcL* and *ITS*, were examined to identify their efficacy for Egyptian mangrove species identification and phylogenetic reconstruction.

*Corresponding author: Email: eglalsaid@arc.sci.eg, eglalmohamed@yahoo.com;

Results: According to pairwise alignments, the *rbcl* region had the highest level of variability (73.2%), whereas the *ITS* region was the least variable (11.96%). The selected Egyptian mangrove species can potentially be distinguished by barcoding loci *rbcl* and *ITS* due to the existence of distinctive variable sites.

Keywords: Mangrove; species; DNA barcode; *rbcl*; *ITS*.

1. INTRODUCTION

Mangroves are woody trees or shrubs that grow in the intertidal zone and are distributed along tropical and subtropical coasts [1]. The word "mangrove" is used to describe 70 species of trees and plants from 20 different families that flourish in areas with high water springs and high tidal levels, according to Jones [2]. These plants are resilient to various environmental challenges, including high salt content, coastal flooding, strong winds, heat, and solar radiation [3]. Their capacity to expand in these conditions is associated with morphological and physiological adaptations, such as stagnation, aerial roots, secondary metabolites and salt excretion mechanisms. Mangrove forests cover approximately 137,760 km² worldwide, of which approximately half are located in Asia alone [4]. Mangrove vegetation contributes to biodiversity conservation, erosion control, and protection from storms and floods along the coast [5]. They provide shelter, coastal protection, habitat, nurseries, and breeding grounds for many fish, crustaceans, and other marine and terrestrial animals [6]. It is also one of the most efficient terrestrial and coastal ecosystems for carbon (C) fixation and storage [7,8]. An acre of growing mangroves can absorb between 50 and 220 metric tonnes of carbon three or four times the amount absorbed by regular forests. However, mangrove forest area worldwide decreases by 1% to 2% annually, due to oil spills and deforestation [9]. In recent years, mangrove reforestation and afforestation have attracted much attention as a strategy to reduce the effects of climate change [10]. In Egypt, mangroves cover around 525 hectares, which are spread out over 28 locations along the country's Red Sea beaches [11]. A large, unconnected runway along the Gulf of Aqaba in the Nabq Protected Area and a small runway in the far south of the Gulf of Suez in the Ras Mohammed National Park [11]. In Egypt, there are two types of mangroves: the red mangrove (*Rhizophora mucronata*) family *Rhizophoraceae* and the black or grey mangrove (*Avicennia marina*) family *Acanthaceae*. Between 30°N and 30°S of the equator, mangrove forests can be

found in tropical climates. The mangrove forests of Egypt are mostly monoecious, including just *Avicennia marina* except for a few sites near the Sudanese port area of Deir al-Masry where *Rhizophora mucronata* coexists alongside *A. marina* [12]. Geographically, Egyptian mangroves can be divided into the Sinai mangrove and the Egyptian-African mangroves that grow on the Red Sea coast [12]. *A. Marina* is relatively more tolerant and adapted to salinity, lower precipitation, and extreme temperature conditions, than *R. mucronata*. This explains the larger global and local distribution (in Egypt) of *A. marina* compared to *R. mucronata*. In Egypt, *R. Mucronata* is only found in a few locations near the Egyptian-Sudanese border (most notably in Marsa al-Shaab and Marsa Abu Fassi). However, there are four different environmental factors that affect mangrove development in Egypt: the climate, the geomorphology of Red Sea lagoons, bays, islands, the qualities of the water, and man-made changes. The main dangers to Egypt's mangroves are human firewood, camel feed, and timber harvesting; pollution, which causes a substantial decline in mangrove biodiversity; and mangrove exploitation for coastal development.

Mangrove management presents a difficult task, particularly when it comes to managing molecular mangroves for long-term sustainability. With the impact of human activity on mangrove ecosystems increasing each year, molecular research on mangrove correlates remains to be conducted. With conventional classification techniques, it is challenging to comprehend the evolutionary relationship among mangrove species. DNA barcoding is a technique that employs short, variable, and standardized DNA regions to assess and classify species. It utilizes a small nucleotide difference at a specific genomic locus of many distinct organisms as a key to classifying many different species [13]. DNA barcoding is presently gaining popularity due to its ease of use and high precision compared to the difficulty and partiality involved with morphology-based taxonomic identification [14]. By enabling quick species identification, DNA barcoding technology may help safeguard

mangrove habitats. ribulose-1,5-bisphosphate carboxylase (*rbcl*), and internal transcription spacer (*ITS*) markers are useful for recognizing mangroves, but they have not been demonstrated as markers for genetic variations within a species [15]. There are still few research articles on DNA barcoding in the mangrove area. For more extensive DNA barcoding applications in ecological research on mangrove vegetation, the *rbcl* and *ITS* markers provide early evaluation data that will be helpful. Tropical and subtropical forests have been the primary focus of previous research on plant DNA barcoding [16,17]. Additionally, the reconstruction of the phylogenetic relationships of particular biological groups using the DNA barcode fragment sequences has emerged in recent years as a new area of study [18-20]. Our knowledge of evolutionary biology and other related fields is improved by this research, which encourages the combination of barcoding technology, ecology, and phylogenetic analysis.

In the present study, two Egyptian mangrove species were assessed through morphological, cytological, and molecular approaches. To evaluate a genetic relationship between studied mangrove species and their relationship to database sequences, two universal DNA barcodes, *rbcl* and *ITS*, were examined to identify their efficacy for the identification and phylogenetic reconstruction of Egyptian mangrove species.

2. MATERIALS AND METHODS

2.1 Study Area

This investigation was carried out during the years (2022 and 2023) in a small mangrove stand grows in a sheltered area interspersed in South Safaga located between the longitudes 26°00'N - 38°00'N, and the latitudes 33°00'E - 59°00'E, with mud flats about 55 feddan in size (44 feddan planted with *Avicennia marina* (Elshora or grey or black mangrove) and about

11 feddan planted with *Rhizophora mucronata* (El Quendel or red mangrove), Fig. 1. The area recorded 11.4 °C during January for the mean minimum temperature and 38.7 °C overall.

2.2 Growth Measurements

The vegetative growth parameters, including total height (cm) and stem diameter (root collar diameter) (cm), were recorded at ages (6 months, 1, 3, and 5 years) from planting in the field. Anatomical studies were also recorded on the main stem. Aiming to study the differences between mangrove forest species that grow along the Red Sea and on the South-eastern tip of the Sinai Peninsula.

2.3 Soil Analysis

Soil chemical properties and some nutrients availability in soil were measured according to Cottenie et al. [21], Tables 1 & 2.

2.4 Histological Studies

Stem sections from one year of *A. marina* and *R. mucronata* species were washed and kept in F.A.A solution for fixation. A series of butanol and ethanol alcohol mixes at varying concentrations were used to induce dehydration. Then, paraffin wax was infused into the dehydrated stem tissues at 50°C for ten days. They were then cut into 15 µ sections using a rotary microtome, dyed with safranin and quick green, and mounted in Canada balsam according to the procedures of Sass [22].

2.5 Experiment design and statistical analysis

A completely randomized design was performed for the experiment. The Student's t-test (*p 0.05) in GraphPad Prism 9 for Windows (GraphPad Software, San Diego, CA, United States) was used to establish the statistical significance of the means.

Table 1. Chemical analysis of soil

Soluble cations (mq/l)				Soluble anions (mq/l)				SP	EC (ds/m)	PH 1:2.5
K+	Na+	Mg++	Ca++	SO4=	Cl	HCO3-	CO3-			
2.25	91.90	59.5	77.5	95.15	128.5	7.5	-	30.0	23.12	7.91

Table 2. Determination of some nutrient availability macro and microelements in soil

Nutrient availability elements (mg/kg)						
N	K	P	Cu	Fe	Mn	Zn
93.0	100.0	9.18	0.05	4.87	1.74	1.08

2.6 DNA Extraction and PCR Reactions

Three typical samples of each *A. marina* and *R. mucronata* from fresh and young leaves were used to extract the complete genomic DNA using the DNeasy plant mini kit (Qiagen). The purity and quantity of the DNA were assessed using spectrophotometry (NanoDrop 2000); Thermo Scientific). The reaction was performed in triplicate using PCR (Polymerase chain reaction) analyses in a T100TM Thermal Cycler (Bio-Rad) with a final volume of 25 µl., 100 ng of genomic DNA, 0.2 mM dNTP, 1x DreamTaq buffer, 1 U of DreamTaq DNA polymerase, and 0.1 M of each primer were used in the PCR amplification process. The DNA sequences identified in the GenBank database were used to generate the primer pairs employed in this study, i.e: *rbcL* F: 5'-ATTACTTGAATGCGACTGCG -3' and *rbcL* R: 5'-GCCAAACATGAATACCACCT-3' and *ITS* F: 5' -ATGCGATACTTGGTGTGAAT- 3' and *ITS* R: 5' -TCCTCCGCTTATTGATATGC- 3' (Fig. 2). The two genes were amplified using the PCR procedure outlined below: after a preliminary denaturation at 95 °C for five minutes, there were

35 cycles that each contained a denaturation step at 94 °C for 45 seconds, an annealing step at 48 °C for 30s, an elongation step at 72 °C for 1.30 minutes, and a final extension step at 72 °C for 10 minutes. The reaction was finally put to an end by keeping the temperature at 4°C. The PCR products were examined using electrophoresis in 2 % agarose gel and a TBE solution (pH 8.0), (Fig. 5). The gel was inspected and kept using the Molecular Imager® GelDocTMXR software.

2.7 PCR Purification and Sequencing

PCR products were electrophoresed on a gel and cleaned using a PCR clean-up kit (Promega, USA). At the (GATC) company in the USA, purified PCR products were directly sequenced from one direction using the ABI 3730xl automated DNA sequencer (Applied Biosystems). The sequences presented in this paper have accession numbers that have been entered into the GenBank database of nucleotide sequences (Table 3).

Table 3. The Accession numbers of Egyptian Mangrove species applied for *rbcL* and *ITS* genes

<i>Species</i>	<i>rbcL</i> Accession number	<i>ITS</i> Accession number
<i>Avicennia marina</i>	LC752949	OQ198465
<i>Rhizophora mucronata</i>	LC752799	OQ390141

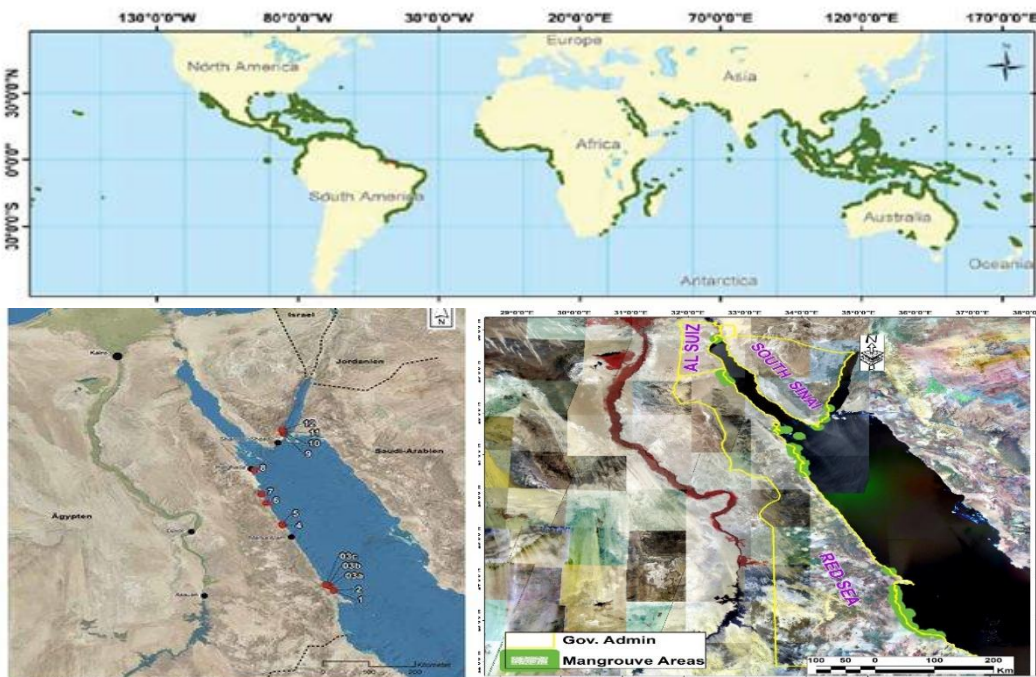


Fig. 1. The figure above shows the distribution of mangroves globally mapped by Giri et al. (2010). Below, Map of Egypt showing the distribution sites of Mangrove species

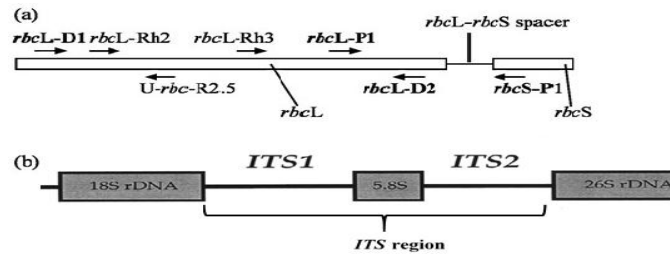


Fig. 2. The structure of a chloroplast *rbcL* and nuclease *ITS* genes and annealing positions of primers used

2.8 DNA Barcoding of *rbcL* and *ITS* Genes

First, the forward sequences were modified using the Basic Local Alignment Tool program, and consensus sequences were obtained (Figs. 6 & 7). The (ClustalW) programme was used to perform multiple sequence alignments. Inferring the evolutionary history was done using the neighbour-joining method [23]. The evolutionary history of the taxa under investigation is thought to be represented by the bootstrap consensus tree generated from 1000 replicates [24]. Branches connected to partitions that had less than 50% of the bootstrap replicates replicate them are collapsed. The percentage of duplicate trees in which related taxa clustered together is shown next to the branches in the bootstrap test (1000 repetitions). The Jukes-Cantor method was used to calculate the evolutionary distances, which are measured in base substitutions per site [25]. The number of segregation sites and nucleotide diversity value, which gauges the average number of nucleotide differences per site between two sequences chosen at random, were determined for *rbcL* and *ITS* using DnaSP v5 [26]. There were four nucleotide sequences in this analysis. All unclear positions for each sequence were deleted (Pairwise deletion option). Evolutionary analyses were performed with MEGA11 [27].

3. RESULTS

In this work, the growth parameters of *Avicennia marina* and *Rhizophora mucronata*, species were evaluated to study the growth differences between the two species, which can withstand and grow well in the arid conditions of the Red Sea. Data in Fig. 3, indicated that the total height of El Quendel or red mangrove (*Rhizophora mucronata*) significantly increased (39.33, 59.33, 84.00, and 136.67 cm) after 6 months, one year, three years, and five years from planting,

respectively, as compared with Elshora or grey or black mangrove (*Avicennia marina*) (19.67, 35.67, 59.33, and 103.33 cm) after six months, one year, three and five years from planting, respectively. Thus, *R. mucronata* recorded the highest value of root collar diameter (1.39, 1.83, 2.67, and 5.96 cm) after ages of six months, one, three, and five years from planting, respectively, as compared with the other mangrove species. While *A. marina* had the smallest root collar diameter (0.40, 0.90, 1.70, and 4.24 cm) after 6 months, one year, three years, and five years, respectively. The results show that *R. mucronata* was superior in growth parameters (total height and stem diameters) as compared with *A. marina*.

Two mangrove species, *Avicennia marina* and *Rhizophora mucronata*, were processed for histological examinations. Transverse section of *A. marina* stem demonstrating the stem's single layer of epidermis and thick cuticle and trichomes covering it, Fig. 4 a. The cortex is divided into two regions. The outer section is made up of collenchyma, which has a small and thick cell wall, while the inner part consists of parenchyma. The collateral bundles are arranged in concentric rings on the eustele stele. Endarch is the Xylem. Circular parenchyma and sclerieds make up the broad pith (Fig. 4a). Transverse sections of *R. mucronata* stem demonstrate that the epidermis reveals a conical appearance made up of variably shaped cells (Fig. 4b). Although the epidermis typically has many layers, a genuine hypodermis with three to seven layers is also typical. The primary cortex is lacunar. Sclerenchymatous idioblasts in the shape of H are visible. Cortex cells have pitted walls and a lot of tannin and oil. Crystals of calcium oxalate are also observed. The vascular bundles are endarch, open, conjoint, and collateral. *Rhizophora mucronata* has rays that are 2-3 cells wide that travel into the xylem. The vessels have perforated plates with scalar form shapes.

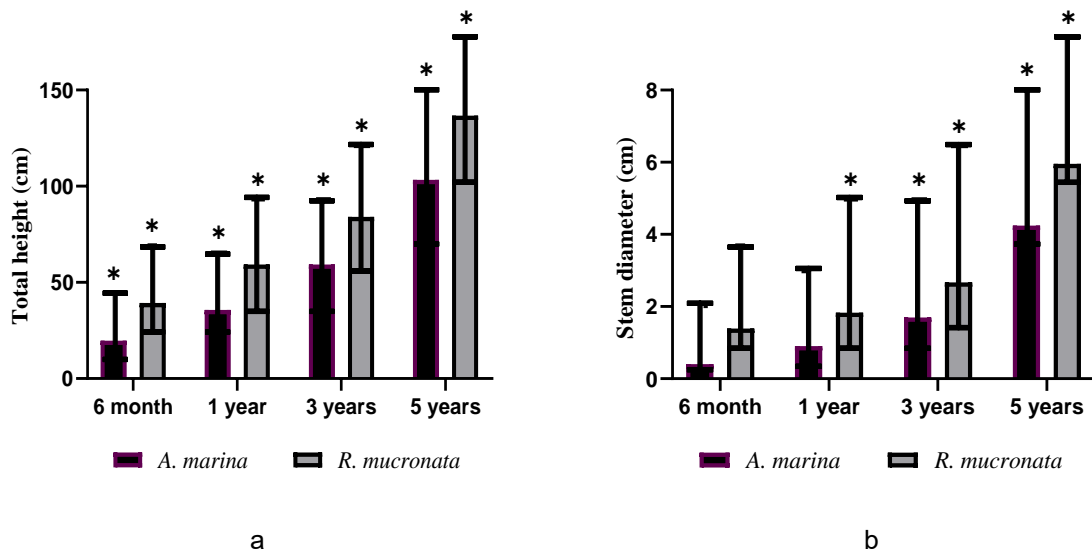


Fig. 3. The growth parameters among Mangroves species in Egypt, a: Total height, b: Stem diameter (Root collar diameter cm). Asterisks (*) indicate statistically significant differences based on Student's t-test ($p < 0.05$)

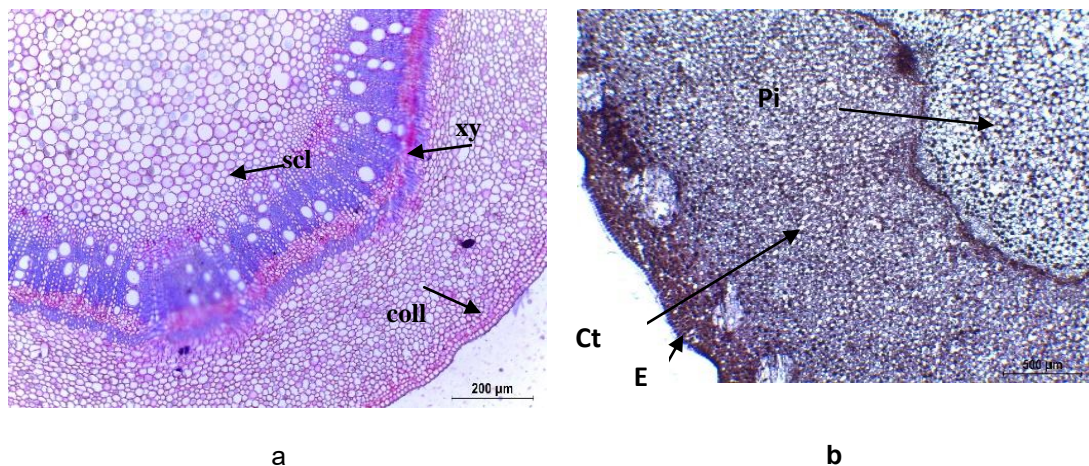


Fig. 4. Transverse section of stem of a: *A. marina*, b: *R. mucronata* showing Vascular bundle, scl: scleried, xy: xylem, coll: collenchyma, Pi: wide pith, Ct: the cortex E: epidermis

3.1 DNA Barcoding of *rbcL* and *ITS* Genes

The amplification products produced by PCR using the two barcoding regions (*rbcL* and *ITS*) for mangrove species, *A. marina* and *R. mucronata*, yielded a single band for each loci (Fig. 5). The PCR product was purified and sequenced, then aligned. The alignment's results are displayed in Figs. (6 & 7), and listed in (Table 4). The accession numbers for each of the new sequences have been deposited in GenBank (Table 3).

3.2 *rbcL* (ribulose-1,5-bisphosphate carboxylase) Sequences

For the two examined species, *rbcL* loci amplification via PCR was successful. The amplified fragments of 389 and 359 bp. for *A. marina* and *R. mucronata* respectively, were obtained with GC contents of 42.41 and 42.89% (Fig. 5). The results of the alignment of the two species are shown in Fig. 6. The similarity between the two species was 95.7%, and the gaps were 2.6%. *rbcL* sequences yielded 359 bp. long sequences after curation with a number of

Indel sites (30) and a nucleotide diversity (P_i) = 0.73, which could differentiate the two Egyptian mangrove species from each other. The two mangrove species' sequences for *rbcL* showed 263 variable sites with 73.2% polymorphism percentages and 96 monomorphic sites with 26.74% polymorphic percentages (Table 4). Therefore, there were 263 singleton variable sites, and two haplotypes (Table 4). Based on the *rbcL* sequence, the maximum likelihood (ML) phylogenetic trees clades of the examined mangrove species with a 100% bootstrap value (Fig. 8).

3.3 Internal Transcription Spacer (*ITS*) Sequences

Successful PCR amplification of the *ITS* loci was obtained for the *A. marina* and *R. mucronata* species, with amplified fragments of 366 and 387 bp, respectively (Fig. 5). The average GC content was 64.75% and 64.02%, respectively. The results of Pairwise Sequence Alignment for two species are shown in Fig. 7. The similarity between the two species was 66.9%, and the gaps were 13.8%. After curation, *ITS* sequences produced 301 bp. -long sequences with a number of Indel sites (86). Within the sequences of the two mangrove species, the *ITS* loci variable sites were 36 sites with 11.96% polymorphic percentages, while the monomorphic sites were 265 and represented 88.03% (Table 4). The number of P_i (nucleotide diversity) = 0.73 and the number of singleton variable sites was 36; hence, two haplotypes were observed (Table 4). These findings demonstrated the effectiveness of the two DNA barcoding techniques in recreating phylogenetic relationships among the mangrove species studied.

Two nucleotide sequences for the loci *rbcL* and *ITS* were examined. According to pairwise alignments. The highest level of variability (73.2%) was found in the *rbcL* region, whereas the *ITS* region was the least variable (11.96%) (Table 4, Figs. 6, 7). The aligned sequences of the *ITS* and chloroplast *rbcL* loci were examined and compared with those in the NCBI database to identify the characteristic sequences that would be used as a useful barcode to distinguish Egyptian mangrove species from other mangrove species. (Table 4, Figs. 6&7).

3.4 Phylogenetic Analyses Using Database Sequences

The individual and combined sequences from the *rbcL* and *ITS* loci were used to estimate trees using the maximum likelihood (ML) algorithm (Figs. 8, 9, and 10). It was shown that the tree constructed based on sequences obtained from *rbcL* loci separated the two Egyptian mangrove species that were gathered in one cluster and grouped with the clade made up of *MT012822 Avicennia marina* and *KF848224 Avicennia officinalis* voucher (Fig. 8). Meanwhile, *Avicennia marina* was placed in a clade with another *Avicennia marina* spp. in genebank species (*KT004471 Avicennia officinalis* voucher, *KT004470 Avicennia marina* voucher, *OK638118 Avicennia marina* subsp. *eucalyptifolia* isolate, and *OK637483 Avicennia marina* isolate) that had the highest average node 100% in the tree created using the sequences from *ITS* loci among the two investigated mangrove species (Fig. 9). Meanwhile, separate another studied species, *R. mucronata*, into a clade composed of *Rhizophora* spp. in the genebank with the average node at 71% (*OK637993 Rhizophora stylosa* isolate, *MZ735368 Rhizophora mucronata* voucher, and *MZ735367 Rhizophora mucronata* voucher). A combined analysis of the two loci, *rbcL* and *ITS*, was compared with data in genebank. This analysis involved 18 nucleotide sequences. All ambiguous positions were removed for each sequence pair (pairwise deletion option). There were a total of 793 positions in the final dataset; evolutionary analyses were conducted in MEGA11 [27]. The tree was constructed using a combined analysis of *rbcL* and *ITS* loci, which separated the two Egyptian mangrove species into two clades. The first clade groups the Egyptian *Avicennia marina* sp. with *MT012822 Avicennia marina*, *KF848224 Avicennia officinalis* voucher, *MZ735367 Rhizophora mucronata* voucher, *OK637990 Rhizophora stylosa* isolate and *OK637993 Rhizophora stylosa* isolate, where the second clade groups *R. mucronata* Egyptian species with *OK637482 Avicennia marina* isolate, *OK637482 Avicennia marina* isolate, *OK638117 Avicennia marina* subsp. *eucalyptifolia* isolate, *OK638118 Avicennia marina* subsp. *eucalyptifolia* isolate, *OK637476 Avicennia marina* isolates, and *KT004471 Avicennia officinalis* voucher (Fig. 10).

Table 4. Molecular characteristics of *rbcl* and *ITS* loci evaluated for two mangrove species, *A. marina* and *R. mucronata*

Barcode	Total Alignment Length (bp.)	No. of monomorphic sites	No. of polymorphic sites	No. of singleton variable sites	No. of Haplotypes	Nucleotide diversity (Pi)	No. of Indel sites
<i>rbcl</i>	359	96	263	263	2	0.732	30
<i>ITS</i>	301	265	36	36	2	0.119	86

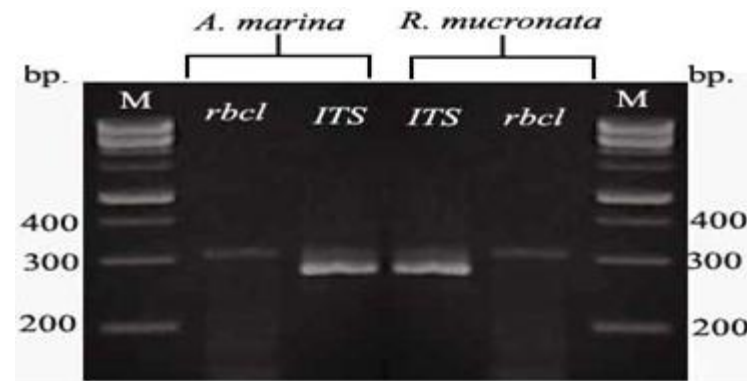


Fig. 5. Agarose gel showing *rbcl* and *ITS* barcoding primers amplification for *A. marina* and *R. mucronata* species. Lane M: 1kb.

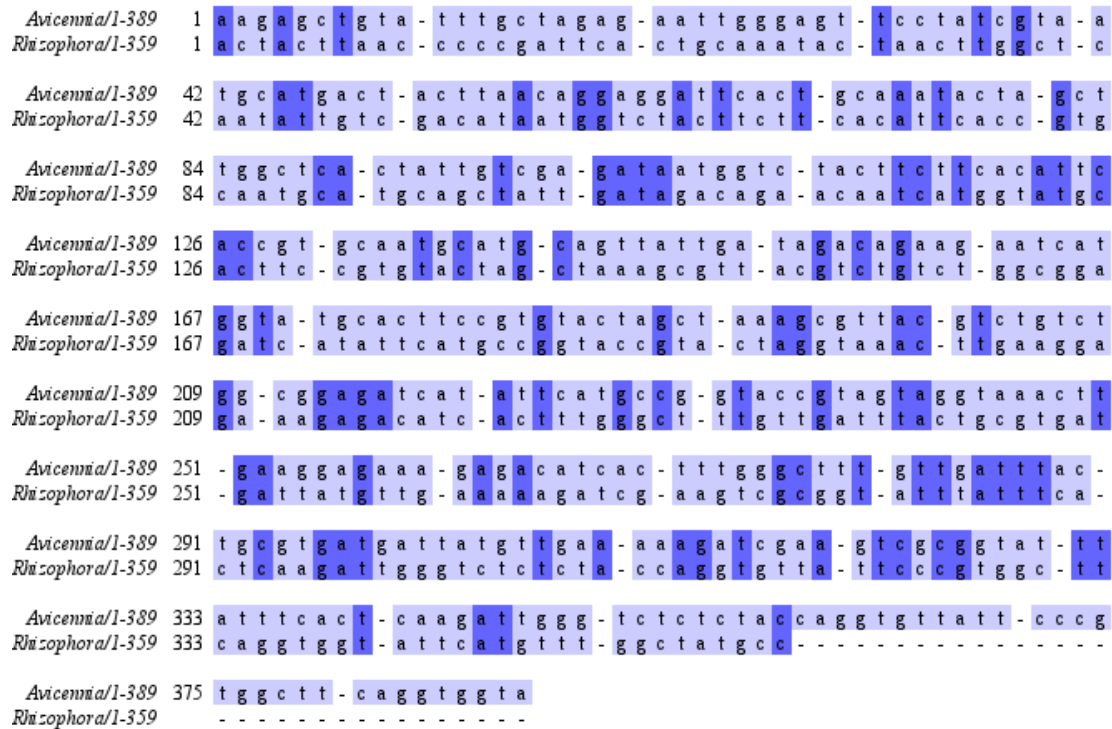


Fig. 6. Sequence alignment of *rbcL* barcoding of studied two mangrove *A. marina* and *R. mucronata*, showing identity regions

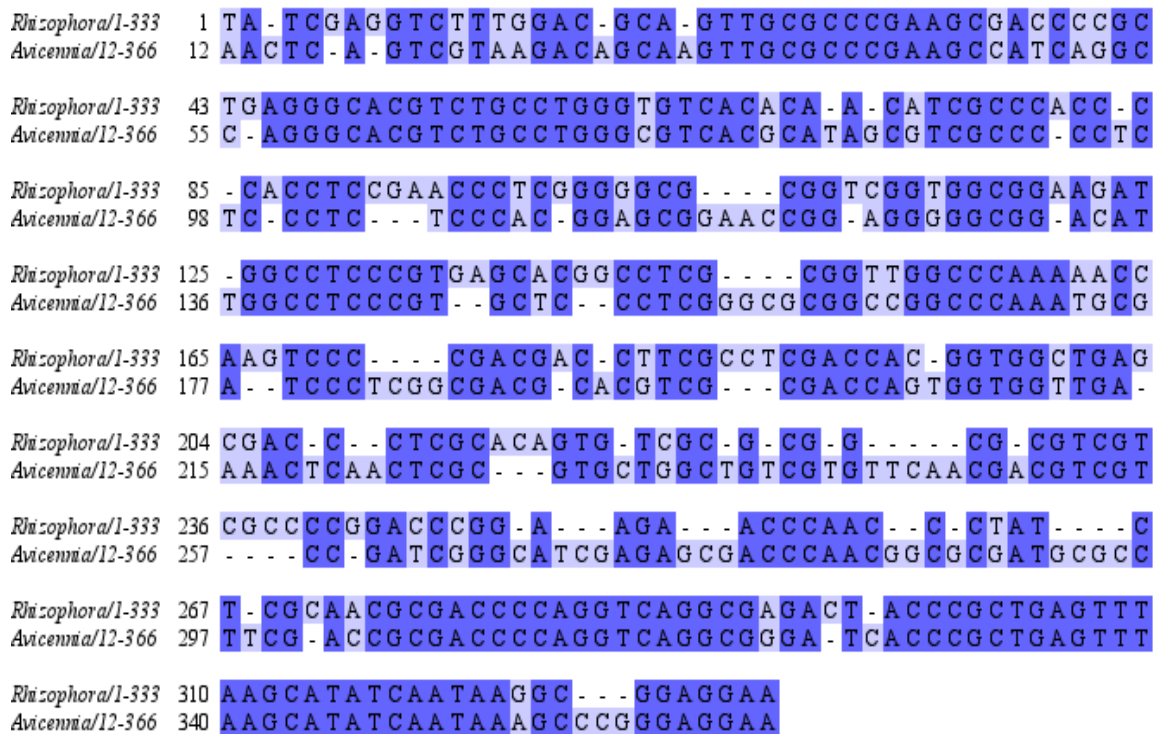


Fig. 7. Sequence alignment of *ITS* barcoding of studied two mangrove *A. marina* and *R. mucronata*, showing identity regions

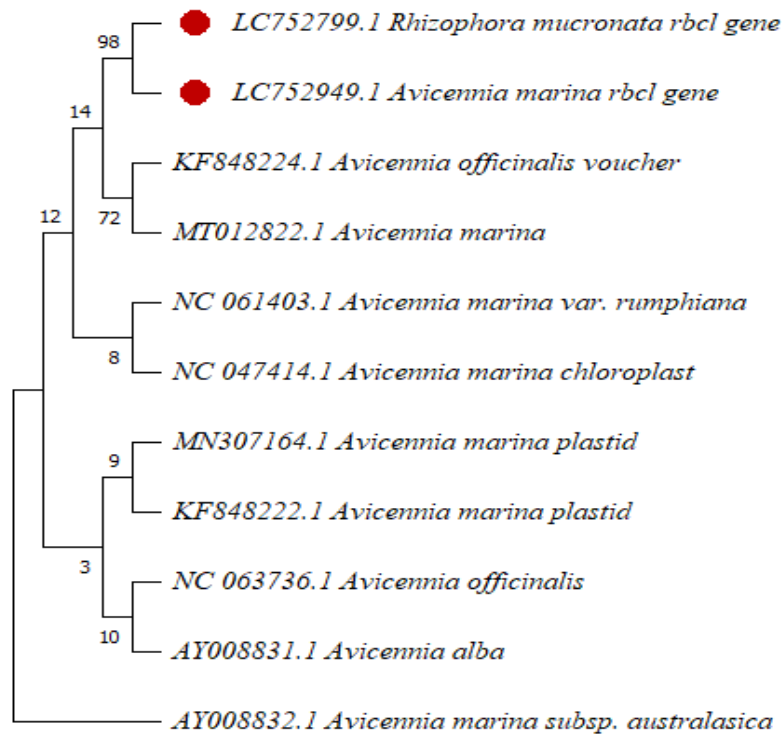


Fig. 8. Phylogenetic tree of *A. marina* and *R. mucronata* species based on *rbcL* sequences. The branches numbers are bootstrap values, the Egyptian mangrove species represented by red typos.

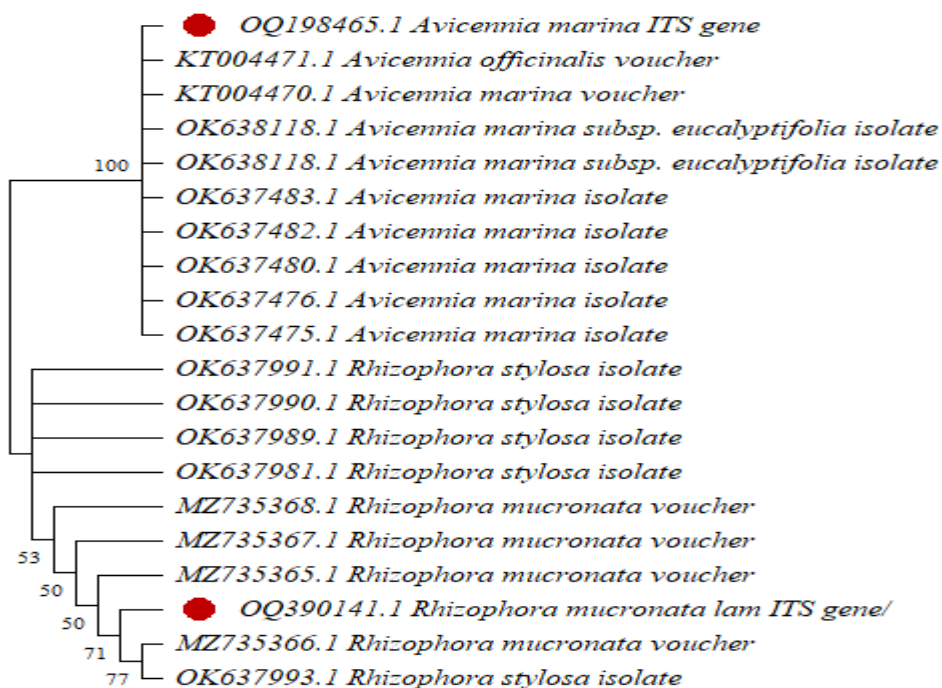


Fig. 9. Phylogenetic tree of *A. marina* and *R. mucronata* species based on *ITS* sequences. The branches' numbers are bootstrap values, red typos represent the Egyptian mangrove species

assessed in terms of primer universality, success rate, and phylogenetic tree construction. The *rbcL* and *ITS* core barcodes of mangrove DNA samples were successfully amplified by PCR and sequenced at 100% success rates. The universality and success rates of our findings were higher than those of Pei [35] with ranges from 90% to 100% in tropical and subtropical forest plant groups. According to earlier research, including that of Tripathi et al. [36], 62.0% of the *ITS* sequences of Indian tropical forest species were successfully sequenced. The success percentage of *ITS* sequencing in the tropical cloud forests of Hainan was 47.20% and 5.76%, according to Kang et al. [37].

Burgess et al. [38] revealed that the barcode could successfully identify 93% of the species in the Canadian flora's temperate zone, while de Vere et al. [39] discovered that *rbcL* + *matK* could recognize 69.4%–74.1% of the blooming plants in Wales, UK. Kress et al. [40] examined 296 woody species in Panama and discovered that *matK* + *rbcL* had a 98% success rate in identifying the species. *rbcL* or *ITS* had a higher identification rate of mangroves this is consistent with previous research results suggested by Li et al. [41] and Sass et al. [42], which suggest the inclusion of *ITS* into the core barcode of plant DNA. Additionally, compared to the chloroplast genes, the nuclear genome's *ITS* region can offer more genetic information from the parents. It has also been shown that specific sections of the chloroplast genome can serve as DNA barcodes in a variety of plant species [43,44]. Recent research has shown that *ITS* and *rbcL* are efficient barcodes for many plant species, either individually or in combination [45,46]. Our *rbcL* and *ITS* locus sequencing results were consistent with those published in CBOL [47]. In the current investigation, the *rbcL* loci were discovered to have more varied sequences than *ITS*. Between the two loci, there was a considerable difference in the number of singleton variable sites, with *rbcL* having the most (263) and the fewest (30) Indel sites. The *ITS* on the other hand, had the fewest singleton variable sites (36) and the most indel sites (86). The large number of segregation sites and subsequent significant nucleotide diversity observed in the studied species are caused by the abundance of species in this genus, and the current data are consistent with earlier observations of this phenomenon in many tropical plant [46]. For greater plant group resolution, it is interesting to note that numerous scientists have suggested merging different barcoding sites or entire

chloroplast genome sequences [48,49]. Several authors have demonstrated the utility of single barcoding loci to differentiate between plant species, including conifers [50] and bamboo [51], wild cherry [52], and zingiber [53]. The results showed that each individual and combination of loci raised the level of discrimination between selected mangrove species. In conclusion, the *ITS* and *rbcL* fragment are suggested for the amplification and sequencing of mangrove plants. We created a phylogenetic tree by comparing *rbcL* and *ITS* sequences from the examined species with those in GenBank (Figs. 8, 9 & 10). Using similar species from a genebank as the outgroup a phylogenetic tree was built to clarify the evolutionary relationship. The phylogenetic tree constructed using *rbcL* loci made it evident that the examined species differed from the outgroup and that all Egyptian species descended from one common ancestor (Fig. 8). Meanwhile, the tree constructed using *ITS* loci separated *A. marina* into a clade composed of another *A. marina* spp. in genebank with the highest average node of 100%. In addition, separate *R. mucronata* in a clade composed of *Rhizophora* spp. in the genebank with the average node at 71%. In various locations, including Barro Colorado Island [40], the Dinghu mountain forest [35], the Ailao mountain forest [54], and tropical cloud forests in Hainan [37], *ITS* and *rbcL* fragments were used for constructing phylogenetic trees. According to the results of the present investigation, it may be possible to enhance the resolution of Egyptian mangrove species by combining and using the individual molecular barcodes obtained from *rbcL* and *ITS* sequences (Figs. 8, 9, and 10). The *rbcL* and *ITS* potential barcode markers in our study all meet the DNA barcoding criteria outlined by Hollingsworth et al. [55]. Due to their appropriateness in terms of sequence variability, they can be utilized to distinguish the studied Egyptian mangrove species [56].

5. CONCLUSION

The preservation of the existing mangrove ecosystems is very important. It is essential to protect existing mangroves while guiding the expansion of their range to support nature-based approaches to climate mitigation and improve the resilience and functionality of these crucial coastal marine ecosystems. The conservation and use of biodiversity depend on mangrove species identification, which is hindered by taxonomic knowledge. Our study investigated the Egyptian mangrove species *Rhizophora*

mucronata and *Avicennia marina*, which grow along the Red Sea and in South Sinai using DNA barcoding technology. To evaluate a genetic relationship between studied mangrove species and their relationship to database sequences, two universal DNA barcodes, *rbcl* and *ITS*, were examined to identify their efficacy for the identification and phylogenetic reconstruction of Egyptian mangrove species.

COMPETING INTERESTS

Authors have declared that no competing interests exist.

REFERENCES

- Poungparn S, Komiyama A, Sangteian T, Maknual C, Patanaponpaiboon P., Suchewaboripont V. High primary productivity under submerged soil raises the net ecosystem productivity of a secondary mangrove forest in eastern Thailand. *Journal of Tropical Ecology*. 2012; 28. DOI: 10.1017/S0266467412000132
- Jones RA. The necessity of the unconscious. *Journal for the Theory of Social Behaviour*. 2002; 32:344-365. DOI:https://doi.org/10.1111/1468-5914.00191
- Spalding M, Kainuma M, Collins L. *World Atlas of Mangroves*. A collaborative project of ITTO, ISME, FAO, UNEP-WCMC, UNESCO-MAB, UNU-INWEH and TNC. London (UK): Earthscan, London. 2010; 319. Available: data.unep-wcmc.org/datasets/22
- Giri C, Ochieng E, Tieszen L, Zhu Z, Singh A, Loveland T, Masek J, Duke N. Status and distribution of mangrove forests of the world using earth observation satellite data. *Global Ecology and Biogeography*. 2010; 154-159.
- Basheer MA, El Kafrawy SB, Mekawy AA. Identification of mangrove plant using hyperspectral remote sensing data along the Red Sea, Egypt. *Egyptian Journal of Aquatic Biology & Fisheries*. 2019;23 (1):27 – 36.
- Alongi D, Chong V, Pfitzner J, Trott LA, Tirendi F, Dixon P, Brunskill G. Sediment accumulation and organic material flux in a managed mangrove ecosystem: Estimates of land-ocean-atmosphere exchange in peninsular Malaysia. *Mar. Geol.*, 2004; 208:383–402.
- Donato DC, Kauffman JB, Murdiyarto D, Kurnianto S, Stidham M, Kanninen M. Mangroves among the most carbon-rich forests in the tropics. *Nat. Geosci*. 2011;4(5):293–297.
- Kristensen E, Bouillon S, Dittmar T, Marchand C. Organic carbon dynamics in mangrove ecosystems: a review. *Aquat. Bot.* 2008;89 (2):201–219.
- FAO. Status and trends in mangrove area extent worldwide. Wilkie, M.L. & Fortuna, S. *Forest Resources Assessment Working Paper No. 63*. Forest Resources Division. Food and Agricultural Organization, Rome, Italy; 2003.
- Sacristán JB, Johansen JB, Duarte CM, Daffonchio D, Hoteitl, McCabe MF. Mangrove distribution and afforestation potential in the Red Sea. *Science of the total Environment*. 2022; 843(15):157098.
- Zahran MA, Willis AJ. *The vegetation of Egypt*. Springer, 2nd edition. 2009; 456.
- PERSGA. Status of Mangroves in the Red Sea and Gulf of Aden. Technical Series Number 11, PERSGA, Jeddah. (Prepared by Khalil ASM). 2004;66.
- Savolainen V, Cowan RS, Vogler AP, Roderick GK, Lane R. Towards writing the encyclopedia of life: an introduction to DNA barcoding. *Philos. Trans. R. Soc. London Ser. B*. 2005;360:1805-1811
- Kress JW. Plant DNA barcodes: Applications today and in the future. *Front. Plant Syst. Evol.* 2017;55(4):291-307.
- Xiaomeng Mao, Wei Xie, Xinnian Li, Suhua Shi, Zixiao Guo. Establishing community-wide DNA barcode references for conserving mangrove forests in China. *BMC Plant Biology*. 2021; 21:571. DOI: https://doi.org/10.1186/s12870-021-03349-z
- Kress WJ, Erickson DL, Swenson NG, Thompson J, Uriarte M, Zimmerman JK. Advances in the use of DNA barcodes to build a community phylogeny for tropical trees in a Puerto Rican forest dynamics plot. *PLoS ONE*; 2010.
- Kress WJ, Wurdack KJ, Zimmer EA, Weigt LA, Janzen DH. Use of DNA barcodes to identify flowering plants. *Proc. Natl. Acad. Sci. USA*. 2014; 102:8369–8374.
- Liao BW, Zhang QM. Area, distribution and species composition of mangroves in China. *Wetl. Sci*. 2014;12:435–440.

19. Newmaster SG, Fazekas AJ, Ragupathy S. DNA barcoding in land Plants: evaluation of rbcL in a multigene tiered approach. *Can. J. Bot.* 2006; 84:335–341.
20. Saddeet AA, Rahul AJ, Kundan K. Assessment of mangroves from Goa, west coast India using DNA barcode. *Springer Plus.* 2016; 5:1554. DOI: 10.1186/s40064-016-3191-4
21. Cottenie A, Verloo M, Kiekens I, Velghe G, Camerlynck R. Chemical analysis of plants and soils. Lab. of Analytical and Agro. State, Univ. Ghent. Belgium; 1982.
22. Sass JE. Botanical micro technique. The low a state Univ. Press, Ames, Iowa. 1964; 228.
23. Thompson JD, Gibson TJ, Higgins DG. Multiple sequence alignment using ClustalW and ClustalX. *Current Protocols in Bioinformatics.* 2003; 1:2-3.
24. Saitou N, Nei M. The neighbor-joining method: A new method for reconstructing phylogenetic trees. *Molecular Biology and Evolution.* 1987; 4: 406-425.
25. Felsenstein J. Confidence limits on phylogenies: An approach using the bootstrap. *Evolution.* 1985; 39:783-791.
26. Theodoridis S, Stefanaki A, Tezcan M, Aki C, Kokkini S, Vlachonasios KE. DNA barcoding in native plants of the Labiatae (Lamiaceae) family from Chios Island (Greece) and the adjacent Cesme-Karaburun Peninsula (Turkey). *Mol. Ecol. Resour.* 2012; 12:620±633. DOI: 10.1111/j.1755-0998.2012.03129.x PMID: 22394710
27. Tamura K, Stecher G, Kumar S. MEGA 11: Molecular evolutionary genetics analysis version 11. *Molecular Biology and Evolution;* 2021. DOI: <https://doi.org/10.1093/molbev/msab120>
28. Almahasheer H, Aljowair A, Duarte CM, Irigoien X. Decadal stability of Red Sea mangroves. *Estuar. Coast. Shelf Sci.* 2016; 169: 164–172.
29. Almahasheer H, Serrano O, Duarte CM, Arias-Ortiz A, Masque P, Irigoien X. Low carbon sink capacity of Red Sea mangroves. *Sci. Rep.* 2017; 7(1):1–10.
30. Charrua AB, Bandeira SO, Catarino S, Cabral P, Romeiras MM. Assessment of the vulnerability of coastal mangrove ecosystems in Mozambique. *Ocean Coast. Manag.* 2020; 189:105145.
31. Quisthoudt K, Schmitz N, Randin CF, Dahdouh-Guebas F, Robert EM, Koedam N. Temperature variation among mangrove latitudinal range limits worldwide. *Trees.* 2012; 26 (6):1919–1931.
32. Burchett MD, Clarke CJ, Field CD, Pulkownik A. Growth and respiration in two mangrove species at a range of salinities. *Physiologia Plantarum.* 1989; 75:299-303.
33. Osland MJ, Feher LC, Griffith KT, Cavanaugh KC, Enwright NM, Day RH, Stagg CL, Krauss KW, Howard RJ, Graces JB, Rogers K. Climatic controls on the global distribution, abundance, and species richness of mangrove forests. *Ecological Monographs.* 2017; 87(2): 341–359.
34. Hebert PD, Cywinska A, Ball SL, DeWaard JR. Proceedings of the Royal Society of London. Series B: Biological Sciences. 2003; 270: 313.
35. Pei NC. Building a subtropical forest community phylogeny based on plant DNA barcodes from Dinghushan plot. *Plant Divers. Resour.* 2012; 34: 263–270. (In Chinese) [CrossRef]
36. Tripathi AM, Tyagi A, Kumar A, Singh A, Singh S, Chaudhary LB, Roy S. The internal transcribed spacer (its) region and trnH-psbA [corrected] are suitable candidate loci for DNA barcoding of tropical tree species of India. *PLoS ONE.* 2013; 8: e57934. [CrossRef] [PubMed]
37. Kang Y, Deng Z, Zang R, Long W. DNA barcoding analysis and phylogenetic relationships of tree species in tropical cloud forests. *Sci. Rep.* 2017;7:12564. [CrossRef] [PubMed]
38. Burgess KS, Fazekas AJ, Kesanakurti PR, Graham SW, Husband BC, Newmaster SG, Percy DM, Hajibabaei M, Barrett SCH. Discriminating plant species in a local temperate flora using the rbcL+matK DNA barcode. *Methods Appl. Fluores.* 2011; 2:333–340. [CrossRef]
39. De Vere N, Rich TC, Ford CR, Trinder SA, Long C, Moore CW, Satterthwaite D, Davies H, Allainguillaume J, Ronca S. DNA barcoding the native flowering plants and conifers of Wales. *PLoS ONE.* 2012; 7:e37945 [CrossRef] [PubMed]
40. Kress WJ, Erickson DL, Jones FA, Swenson NG, Perez R, Sanjur O, Bermingham E. Plant DNA barcodes and a community phylogeny of a tropical forest dynamics plot in Panama. *Proc. Natl. Acad. Sci. USA.* 2009; 106: 18621–18626. [CrossRef]

41. Li DZ, Gao LM, Li HT, Wang H, Ge XJ, Liu JQ, Chen ZD, Zhou SL, Chen SL, Yang JB. Comparative analysis of a large dataset indicates that internal transcribed spacer (its) should be incorporated into the core barcode for seed plants. *Proc. Natl. Acad. Sci. USA.* 2011;108:19641–19646.
42. Sass C, Little DP, Stevenson DW, Specht CD. DNA barcoding in the cycadales: Testing the potential of proposed barcoding markers for species identification of cycads. *PLoS ONE.* 2007; 7, 2: e1154. [CrossRef] [PubMed]
43. Li X, Yang Y, Henry RJ, Rossetto M, Wang Y. Plant DNA barcoding: from gene to genome: Plant identification using DNA barcodes. *Biological Reviews.* 2015; 90: 157-166. DOI: 10.1111/brv.12104
44. Wu F, Li M, Liao B, Shi X, Xu Y. DNA barcoding analysis and phylogenetic relation of mangroves in Guangdong Province, China. *Forests.* 2019; 10(1): 56. DOI: 10.3390/f10010056
45. Hollingsworth PM, Forrest LL, Spouge JL, Hajibabaei M, Ratnasingham S. A DNA barcode for land plants. *Proceedings of the National Academy of Sciences of the United States of America.* 2009; 106:12794-12797. DOI:10.1073/pnas.0905845106.
46. de Melo Moura CC, Brambach F, Jair Bado KJH, Krutovsky KV, Kreft H. Integrating DNA barcoding and traditional taxonomy for the identification of Dipterocarps in Remnant Lowland Forests of Sumatra. *Plants.* 2019; 8 (11):461. DOI:10.3390/plants8110461.
47. CBOL Plant Working Group. DNA barcode for land plants. *Proceedings of the National Academy of Sciences of the United States of America.* 2009;106: 12794-12797. DOI: 10.1073/pnas.0905845106
48. Girma G, Spillane C, Gedil M. DNA barcoding of the main cultivated yams and selected wild species in the genus *Dioscorea*. *Journal of Systematics and Evolution.* 2016; 54: 228-237. DOI: 10.1111/jse.12183
49. Gogoi B, Wann SB, Saikia SP. DNA barcodes for delineating *Clerodendrum* species of North East India. *Scientific Reports.* 2020;10: 13490. DOI: 10.1038/s41598-020-70405-3
50. Pham MP, Tran VH, Vu DD, Nguyen QK, Shah SNM. Phylogenetics of native conifer species in Vietnam based on two chloroplast gene regions *rbcL* and *matK*. *Czech Journal of Genetics and Plant Breeding.* 2021; 57: 58-66. DOI: 10.17221/88/2020-CJGPB
51. Dev SA, Sijimol K, Prathibha PS, Sreekumar VB, Muralidharan EM. DNA barcoding as a valuable molecular tool for the certification of planting materials in bamboo. *Biotech.* 2020; 10(2): 59. DOI: 10.1007/s13205-019-2018-8
52. Unsal SG, Ciftci YO, Eken BU, Velioglu E, Marco GD. Intraspecific discrimination study of wild cherry populations from North-Western Turkey by DNA barcoding approach. *Tree Genetics and Genomes.* 2019; 15:16. DOI:10.1007/s11295-019-1323-z
53. Saha K, Dholakia BB, Sinha RK. DNA barcoding of selected *Zingiberaceae* species from North-East India. *Journal of Plant Biochemistry and Biotechnology.* 2020; 29:494-502. DOI: 10.1007/ s13562-020-00563-y
54. Lu MM, Ci XQ, Yang GP, Li J. DNA barcoding of subtropical forest trees—A study from Ailao mountains nature reserve, Yunnan, China. *Plant Divers. Resour.* 2013; 35:733–741.
55. Hollingsworth PM, Graham SW, Little DP. Choosing and using a plant DNA barcode. *PLoS One.* 2011;6(5): e19254. DOI: 10.1371/journal.pone.0019254
56. Kumar S, Stecher G, Tamura K. MEGA7: molecular evolutionary genetics analysis version 7.0 for bigger datasets. *Mol Biol Evol.* 2016; 33:1870–4.

© 2023 Said and Bahnasy; This is an Open Access article distributed under the terms of the Creative Commons Attribution License (<http://creativecommons.org/licenses/by/4.0>), which permits unrestricted use, distribution, and reproduction in any medium, provided the original work is properly cited.

Peer-review history:

The peer review history for this paper can be accessed here:
<https://www.sdiarticle5.com/review-history/100871>